Ultimate Moment Capacity of Thin-walled Cold-formed Members of Vehicular Structures

Frank Monasa

Timothy Chipman

ULTIMATE MOMENT CAPACITY OF THIN-WALLED COLD-FORMED MEMBERS OF VEHICULAR STRUCTURES

by

Frank Monasa* and Timothy Chipman**

INTRODUCTION

The framing system of the passenger compartment of small buses (16-19 passengers) is constructed from a variety of members of thin-walled cold-formed sections, as shown in Fig. 1. In evaluating the structural strength capacity of passenger compartment structures in impact situations, an elastic-plastic analysis (1,6) was used to determine the ultimate load carrying capacity and the collapse characteristics of the framing system of the passenger compartment. In this method of analysis, it was required to determine the ultimate moment capacity of the thin-walled cold-formed structural members. Due to the three-dimensional analysis of the structure and the application of arbitrary loads, it was necessary to determine the ultimate moment capacity of these members with respect to the strong and weak bending axes of the section under an arbitrary (either positive or negative) bending moment, as well as the ultimate torsional moment capacity. Methods exist (2,7 and 11), based on analytical and experimental results, that predict the ultimate moment capacity of thin-walled sections. However, these methods are only applicable to limited type of cross sections, and to a specified application of the bending moment. Winter (11) reported the results of an extensive experimental investigation of the strength of thin steel stiffened and unstiffened compression flanges. He presented a formula for computing the effective width b for stiffened plates along both longitudinal edges. Later this formula was incorporated in the AISI Specification (8). Winter in his commentary on the 1968 edition of the AISI Specification (10) presented detailed analysis of thin-walled cold-formed sections, their buckling behavior and post buckling strength. Dawson and Walker (2) proposed a method for the design of thin-walled beams and determining their collapse moment. An equation for the collapse moment of a lipped-channel section was derived. It was assumed that: 1 - the section is acted upon only by pure moment so that the top flange is under uniform compression, and 2 - the web was fully yielded (which may not be true). In the expression for the collapse moment, the ultimate stress, f_{ult}, in the top flange and the entire width of flange were used to obtain the forces in the flange. Reck, Pekoz, and Winter (7) studied the inelastic reserve strength of cold-formed steel beams whose compression flanges are stiffened along both longitudinal edges by webs. Three different hat sections were considered in this study whose top flanges were under uniform compression. Equations for the ultimate moment of the section were derived for sections with and without yielded tension flange at ultimate moment. It was concluded that the inelastic reserve strength depends on: 1 - the ultimate strain capacity of the compression flange, 2 - the location of the neutral axis, 3 - the

---

* Associate Professor, Civil Engineering Department, Michigan Technological University, Houghton, Michigan.

** Staff Engineer, Bechtel Corporation, Ann Arbor, Michigan.

relative magnitude of the web area as compared to the flange areas and 4 - due to partial plastification of the section. Kalyanaraman, Pekoz, and Winter (3) studied the elastic local buckling and post-buckling behavior of unstiffened elements under uniform compression in order to develop an effective width equation for unstiffened elements and examined the distortion of the section in the post-buckling range. Series of tests were conducted using cold-formed steel stub columns, long columns, and beams. It was observed that the failure of an unstiffened element occurs when the maximum compressive stress at the supported edge of the element reaches the yield strength, f_y, of the material. Kalyanaraman and Pekoz (4) presented an analytical solution to the elastic and inelastic local buckling and post-buckling behavior of unstiffened elements under uniform compression stresses. An equation for the effective width of unstiffened compression element was derived, and the analytical solution was compared with test results. Yener and Pekoz (12) investigated the inelastic load carrying capacity of cold-formed steel beams with stiffened compression flanges, and developed experimentally a failure criterion based on the ultimate compressive strain for hat and channel section beams under uniform moment and moment gradient.

In this paper, a simplified method has been developed that combines tests and analytical results to predict the ultimate moment capacity of a general thin-walled cross section. Simplified equations were obtained using test results, based on other studies (2,9), that predict the post-buckling strength and ultimate strength capacity of stiffened and unstiffened compression plate elements.

ULTIMATE STRENGTH OF THIN-WALLED SECTIONS

In the engineering bending theory, it is assumed that there is no change in the cross-section of flexural members during loading. This assumption is valid when beams are of compact sections. However, with certain cold-formed thin-walled members, significant elastic local buckling of one or more of the compression plate elements of the cross-section may occur, and the elements can often sustain additional compression stresses in the post-buckling range but do fail when yielding initiates. Therefore, in order to determine the ultimate moment capacity of these members, the local buckling effect and the post buckling behavior of the compression plate elements must be considered. If the flat width to thickness ratio, w/t, is sufficiently large the flange will buckle under a compressive stress equal to critical buckling stress, f_{cr}. This buckling does not indicate failure of either the flange or of the entire section due to the post-buckling behavior of thin-walled sections. After buckling the stress distribution across the compressive plate element becomes non-uniform, and eventually yield occurs at the edges of the element. However, compression flanges with small w/t ratios continue to carry their compression load after initial yielding is reached, and while yielding spreads into the web, resulting in inelastic reserve strength.

DETERMINATION OF ULTIMATE MOMENT OF THIN-WALLED SECTIONS

Thin-walled sections consist of flat plate elements continuously connected along their mutual edges. Therefore, the section can be considered as being made up of an assembly of individual plates with relevant boundary and loading conditions. The boundary conditions require equilibrium of moments and shear forces as well as compatibility of edge displacement and rotation between adjacent plates. Due to the complexity of the application of these boundary conditions in the analysis of thin-walled section, the AISI Specification (8) assumes simply supported edges for the plate elements of a section, therefore, there are no forces transmitted across the boundaries. Each plate element of the cross-section is placed into one of two categories: stiffened elements and unstiffened elements as shown in Fig. 2.

Assumptions

Several assumptions are made in order to simplify the procedure of predicting the ultimate moments, M_{ult}, of thin-walled sections. These assumptions are: 1 - elements or parts of elements in compression, caused by bending, will resist an average compressive stress equal to the ultimate stress, f_{ult} (based on the full flat width of the element) which is obtained when the edge membrane stress first reaches the yield stress, f_y. Thus the collapse mechanism is a localized effect occurring at the cross-section. Therefore, once the average stress in the compressive element reaches f_{ult} the element will not resist further stress and additional moment is resisted as yield spreads through the webs. 2 - the material is assumed to be elastic-perfectly plastic. 3 - elements or parts of elements in tension, caused by bending, will resist a tensile stress equal to the yield strength of the material. 4 - the resisting ultimate moment is calculated using the initial cross-section geometry before buckling occurs.

Procedure

a. Ultimate Bending Moment Capacity

Ultimate stress criteria for stiffened elements under uniform compression, developed by Dawson and Walker (2), and for unstiffened elements under uniform compression, presented by Yu (9), were used to determine the ultimate stress, f_{ult}, in a compressive element based on the full flat width of the element. Graphs (Fig. 3a, and Fig. 3.30) that are presented in Refs. (2 and 9), respectively, are shown in Figs. 3 and 4, however, they have been approximated by straight lines to simplify the computations. The equations of the straight line approximation for stiffened elements are:

$$f_{ult}/f_y = 1 \qquad \sqrt{f_y/f_{cr}} < 0.65 \qquad (1a)$$

$$f_{ult}/f_y = 1.42 - 0.64\sqrt{f_y/f_{cr}} \qquad 0.65 < \sqrt{f_y/f_{cr}} < 1.65 \qquad (1b)$$

$$f_{ult}/f_y = 0.45 - 0.065\sqrt{f_y/f_{cr}} \qquad 1.65 < \sqrt{f_y/f_{cr}} < 5.0 \qquad (1c)$$

and for unstiffened elements:

$$f_{ult}/f_y = 1 \qquad (w/t)\sqrt{f_y} < 63.33 \qquad (2a)$$

$$f_{ult}/f_y = 1.27 - 4.34E\text{-}0\,3(w/t)\sqrt{f_y} \qquad (w/t)\sqrt{f_y} > 63.33 \qquad (2b)$$

To use Fig. 3, the flat width to the thickness ratio, w/t, is required in order to determine the elastic critical buckling stress, f_{cr}, for stiffened element. Then the ratio f_y/f_{cr} is found and the ratio of f_{ult}/f_y is obtained from the figure. For unstiffened element the value of $(w/t)\sqrt{f_y}$ is calculated and the ratio of f_{ult}/f_y is determined from Fig. 4.

To determine the ultimate moment capacity, the section is assumed to be in a positive bending mode about the strong axis (local 3-axis as shown in Fig. 5, i.e., compression above the neutral axis). The first estimate of the plastic (ultimate) neutral axis location is assumed to be that of the centroidal axis. The compressive force is then calculated by multiplying the ultimate strength, f_{ult}, or yield strength; f_y, (depending on the w/t ratio) of each element above the centroidal axis by its respective area. And the tensile force is calculated by multiplying the yield strength of the material by the respective area of each plate element below the centroidal axis. The neutral axis is then moved upward or downward until equilibrium of forces is attained. Then, the ultimate moment is calculated by summation of the moment of forces in each plate element about the neutral axis. This procedure is then repeated for a negative bending moment mode about the strong axis (local 3-axis). The above procedure is repeated for bending about the weak axis (local 2-axis, as shown in Fig. 5) of the section.

b. Ultimate Torsional Moment Capacity

To determine the ultimate torsional moment capacity, it is assumed in addition to the previous assumptions that warping of the cross-section will not affect the ultimate shearing strength of the section in torsion. Torsion will cause primarily shear stresses in the cross-section, consequently, the ultimate torsional moment depends on the ultimate shearing strength of each plate element of the cross-section.

When a plate element with a relatively small w/t ratio is subjected to shear stress, it will probably fail in shear yielding beginning at the neutral axis at an ultimate shearing strength, τ_{ult}, of about τ_y, where,

$$\tau_y = f_y / \sqrt{3} \qquad w/t < 380/\sqrt{f_y} \tag{3a}$$

For plates having moderate w/t ratios, the ultimate shearing strength is equal to the inelastic shear buckling stress, τ_{icr}, which can be obtained from (9) as follows:

$$\tau_{icr} = \sqrt{0.8\, f_y\, \tau_{cr}/\sqrt{3}} \qquad 380/\sqrt{f_y} < w/t < 547/\sqrt{f_y} \tag{3b}$$

where τ_{cr} is the initial elastic critical shear buckling stress obtained from Eq. (3c). For plates with large w/t ratios, the element will fail in shear buckling at an ultimate shear stress equals to the initial elastic critical shear buckling stress, τ_{cr}, where

$$\tau_{cr} = \frac{k\,\pi^2\,E}{12(1-\nu^2)(w/t)^2} \qquad w/t > 547/\sqrt{f_y} \tag{3c}$$

where k is the buckling coefficient in shear. For a long plate, k is equal to 5.35 for simply supported elements and 8.98 for fixed supports (9). In this study, plate elements are assumed to be simply supported, i.e., k = 5.35. E is the Young's modulus of the material and ν is Poisson's ratio.

To calculate the ultimate torsional moment, the ultimate shear strength is determined first for each element in the cross-section based on Eqs. (3a, 3b, and 3c). For open cross-sections, the ultimate torsional moment is found by assuming that each element of the cross-section is stressed at its ultimate shearing strength. Then from membrane analogy, the ultimate torsional moment, T_{ult}, for a thin rectangular plate element of width w and thickness t can be obtained from:

$$T_{ult} = \frac{1}{2} w\, t^2\, \tau_{ult} \tag{4}$$

The ultimate torsional moment for an open cross-section will be equal to the summation of the ultimate torsional moment of its rectangular plate components. For closed cross-sections, the ultimate shearing strength of each element is obtained, and the entire cross-section is then assumed to be stressed at the average of the ultimate shearing strength of the elements. From membrane analogy, the ultimate torsional moment, T_{ult}, can be obtained as follows:

$$T_{ult} = 2\, a\, b\, t\, \tau_{ult} \tag{5}$$

Where a and b are the centerline dimensions of the cross-section.

COMPUTER PROGRAM, PROP

A computer program (PROP), developed in this study, was written to determine the ultimate bending and torsional moment capacity of thin-walled steel sections, using the procedure described above, as well as the elastic properties, i.e., area, torsional rigidity, moment of inertia, etc.). The flow diagram for PROP is shown in Figs. 6a and 6b. A typical computer output for the element's sectional properties and ultimate (or plastic) moments is shown in Fig. 7.

The input of PROP consists of the yield stress, f_y, Young's modulus, E, and Poisson's ratio, ν, of the steel used, the coordinates of the end points, thickness, and radius of bend of each element. The local coordinates correspond to orthogonal coordinate system whose X-axis is parallel to the local 1-axis and Z-axis is parallel to the local 3-axis (see Fig. 5).

A critical portion of program PROP is the routine that determines the location of the ultimate (or plastic) neutral axis. The program is developed for general section geometry. Therefore, the method used for determining the ultimate neutral axis location must also be for a general section. The method uses the centroidal axis as the first estimate of the ultimate neutral axis. The compressive and tensile forces in the cross-section are calculated as well as the resultant moment. If the tensile and compressive forces are within 1% of each other, equilibrium of forces is assumed to be attained. Then the procedure is stopped and the calculated resultant moment is the ultimate bending moment. If the forces are not within 1% of each other, the position of the neutral axis is moved by an incremental value until equilibrium of forces is attained. This process is repeated until the forces are within 1% of each other or 20 iterations occur. If the direction that the neutral axis must be moved changes direction, the incremental value is divided by 2 to find a new incremental value.

TESTS RESULTS

To verify and check the reliability of the results predicted from the analytical method used in this study, an experimental procedure was carried out (1,6), and the test results were compared with the results obtained from the analytical procedure.

Three different sections, as shown in Fig. 8, were loaded as cantilever beams to determine the ultimate bending moment capacity of each section, and to study the behavior of the section when loaded beyond its ultimate moment. The test specimens were 25 - 30 inches (63-76 cm.) long with a hole drilled in one end for the loading pin. The other end was placed in a 6 inch (15 cm.) square box support. Several hardwood blocks, cut to the shape of the cross-section, were forced around the section inside the box support. This support, then, was rigidly connected to the base of a portable hydraulic lift. The beams were then loaded using the hydraulic jack on the lift. The loads were measured with an electronic load cell, and deflections were measured at the load pin by an electronic potentiometer and manually to ensure accuracy of the measurements. Tests were performed for positive and negative bending about the strong and weak axes. To study the behavior of the moment-hinge rotation characteristics of the sections, the load-deflections data, obtained from the cantilever tests, was used. In these tests it was assumed that: 1. The failure is restricted to a localized portion of the beam. 2. The flexibility of the beam remains constant, except at the location of the hinge. 3. The deflection at the tip of the beam is due to elastic deformations plus rigid body rotation of the beam caused by the rotation of the hinge. 4. Elastic deformations remain small so that shortening of the lever arm is due only to rigid body rotation of the beam.

The deflection due to the hinge rotation can then be determined by subtracting the elastic deformations from the deformations measured during the test. The elastic deformations at any load can be found by determining the flexibility of the beam from the linear portion of the load-deflection curve and multiplying it by the corresponding load. From Fig. 9, it can be seen that the hinge rotation, ϕ, is:

$$\phi = \sin^{-1} [\delta_t - \delta_e)/L] \qquad (6)$$

where δ_t and δ_e are the total and elastic deflections at the free end, respectively. And the moment, M, corresponding to the hinge rotation can then be determined from:

$$M = P\ L \cos \phi \qquad (7)$$

where P is the end load.

Typical moment-hinge rotation behavior for bending tests is shown in Figs. 10 to 13. The ultimate moments predicted by program PROP, using the actual yield strength and modulus of elasticity for teach section, were also plotted on the corresponding figure.

SUMMARY AND CONCLUSIONS

In this paper, an approximate analytical method, and a computer program, PROP, were developed to determine the ultimate bending and torsional moment capacity of thin-walled sections of an arbitrary geometry.

The method predicted moment values for sections bent about their strong axis, except for the zee section, close to those determined experimentally. Test results of sections bent about their strong axis indicated that the test specimens attained approximately a constant moment, in general, just slightly smaller than the ultimate moment. However, Miles (5) showed for very thin-walled sections that the ultimate moment drops extensively as rotation of the plastic hinge increases. When the sections were bent about their weak axis, the predicted analytical results were higher by about 18% than the test results. This is probably due to the effect of the twisting moment which was induced in the test specimen; because the load was not applied at the shear center of the section. The analytical method of determining the ultimate moments predicted, for beams of zee sections, values higher than those of the experimental procedure by about 30%. This might be due to problems during testing caused by bi-axial bending induced in the section due to the applied load.

ACKNOWLEDGEMENT

This paper is a part of a research that was conducted in Michigan Technological University on the engineering analysis of the structural integrity of small buses. The financial support of the Michigan Department of Transportation is greatly appreciated.

APPENDIX I - REFERENCES

1. Chipman, T., "Elastic-Plastic Analysis of Flexible Frames," A thesis submitted in partial fulfillment of the requirements for the degree of Master of Science in Civil Engineering, Michigan Technological University, 1981, 109 pages.

2. Dawson, R. G., and Walker, A. C., "A Proposed Method for the Design of Thin-Walled Beams Which Buckle Locally," The Structural Engineer, Vol. 50, No. 2, Feb. 1972, pp. 95-105.

3. Kalyanaraman, J., Pekoz, T., and Winter, G., "Unstiffened Compression Elements," Journal of the Structural Division, ASCE, Vol. 103, No. ST9, Proc. Paper 13197, Sept., 1977, pp. 1833-1848.

4. Kalyanaraman, V., and Pekoz, T., "Analytical Study of Unstiffened Elements," Journal of the Structural Division, ASCE, Vol. 104, No. ST9, Proc. Paper 14028, Sept., 1978, pp. 1507-1524.

5. Miles, J. C., "The Determination of Collapse Load and Energy Absorbing Properties of Thin-Walled Beam Structures Using Matrix Methods of Analysis," International Journal of Mechanical Sciences, Vol. 18, Nos. 7 & 8, 1976, pp. 399-405.

6. Monasa, F., "Engineering Analysis of the Structural Integrity of Small Buses," Report submitted to the Michigan Department of Transportation, Contract No. 79-2533, Nov. 1981, 334 pages.

7. Reck, H. P., Pekoz, T., and Winter, G., "Inelastic Strength of Cold-Formed Steel Beams," Journal of the Structural Division, ASCE, Vol. 101, No. ST11, Proc. Paper 11713, Nov., 1975, pp. 2193-2203.

8. Specification for the Design of Cold-Formed Steel Structural Members, American Iron and Steel Institute, 1968.

9. Yu, Wei-Wen, Cold-Formed Structures, McGraw-Hill, New York, N.Y., 1973, pp. 53-102.

10. Winter, G., "Commentary on the 1968 Edition of the Specification for the Design of Cold-Formed Steel Structural Members," American Iron and Steel Institute, Washington, D.C., 1968.

11. Winter, G., "Strength of Thin Steel Compression Flanges," Transactions, ASCE, Vol. 112, Paper No. 2305, 1947, pp. 527-576.

12. Yener, M., and Pekoz, T., "Inelastic Load Carrying Capacity of Cold-Formed Steel Beams," Proceedings of the Fifth International Specialty Conference on Cold-Formed Steel Structures, November 18-19, 1980, University of Missouri-Rolla, pp. 145-174.

13. AISI Guide for Preliminary Design of Sheet Steel Automotive Structural Component, 1981.

APPENDIX II - NOTATION

a,b = centerline dimensions of thin-walled closed sections,

E = Young's modulus,

f_{cr} = critical buckling stress

$$= \frac{k\pi^2 E}{12(1-\nu^2)(w/t)^2}$$

f_{ult} = ultimate strength,

f_y = yield strength,

k = buckling coefficient,

L = span length of cantilever beams,

M_{ult} = ultimate bending moment capacity,

P = point load at the free end of cantilever beams,

T_{ult} = ultimate torsional moment capacity,

t = thickness of plate elements,

w = flat width of plate elements,

δ_e = elastic deflection at free end of beams,

δ_t = total deflection at free end of beams,

ϕ = hinge rotation,

τ_{cr} = elastic critical shear buckling stress,

τ_{icr} = inelastic shear buckling stress,

τ_{ult} = ultimate shear stress,

τ_y = yield shear stress,

ν = Poisson's ratio.

Fig. 1 - STRUCTURAL ELEMENT SECTIONS - BUS A

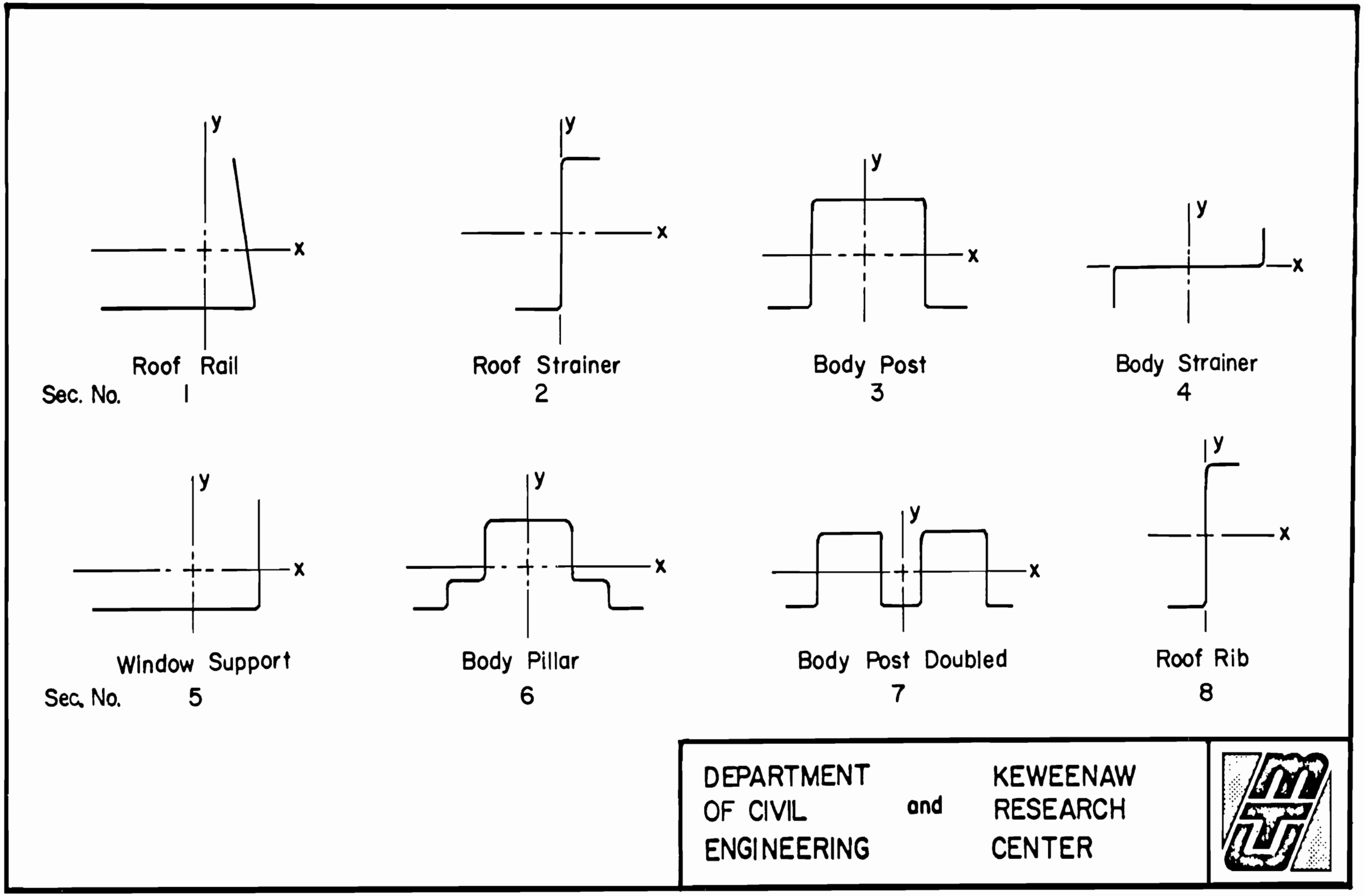

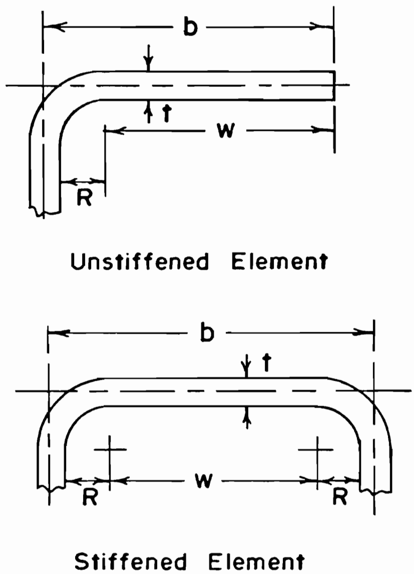

b - length of element

w - flat width of element

R - radius of bend

t - thickness

Fig. 2 - Stiffened and Unstiffened Elements

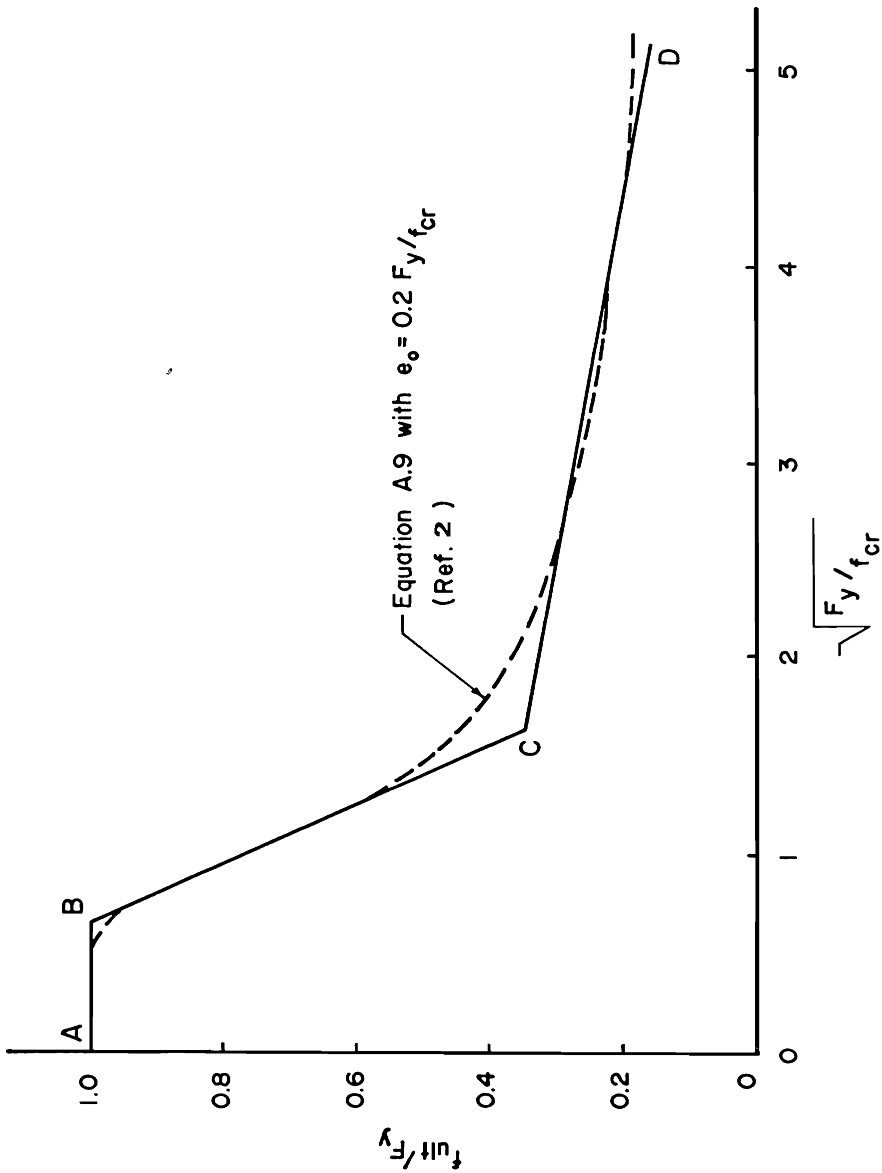

Fig. 3 - Predicted ultimate stress for stiffened compression elements

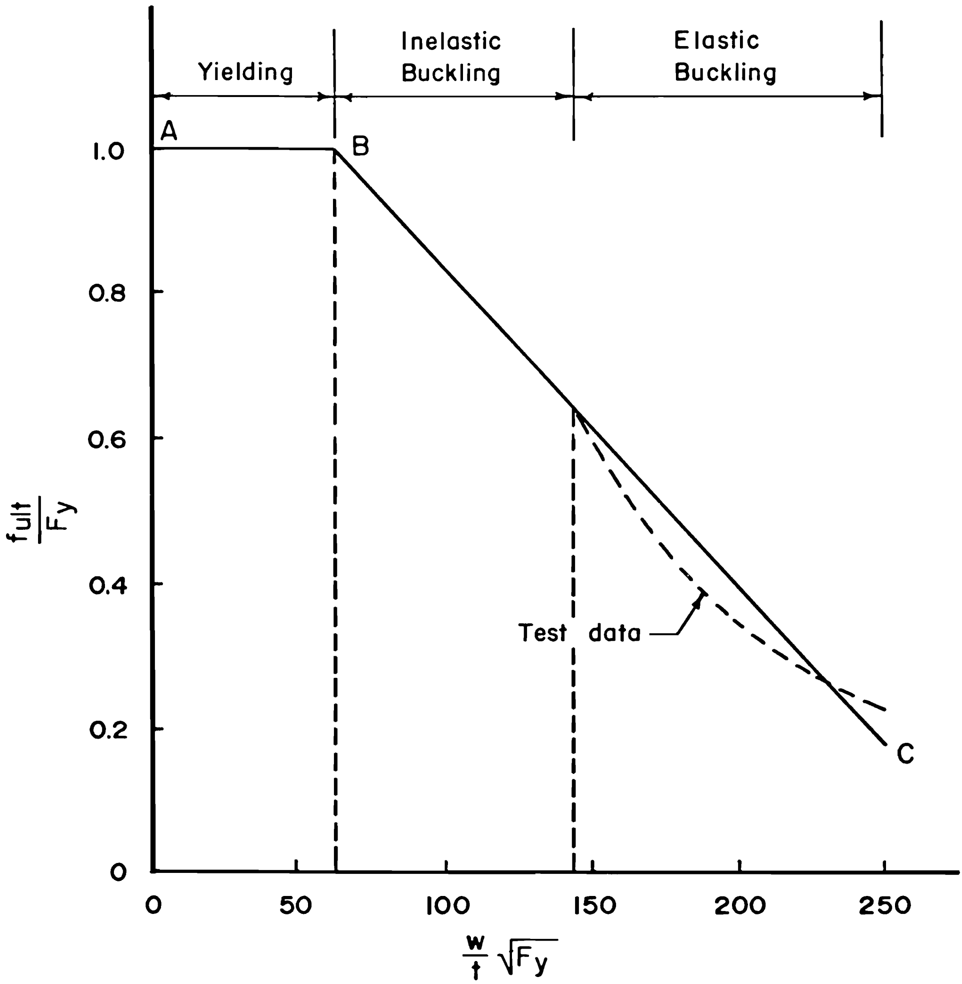

Fig. 4 - Predicted maximum stress for unstiffened compression elements (Ref. 9)

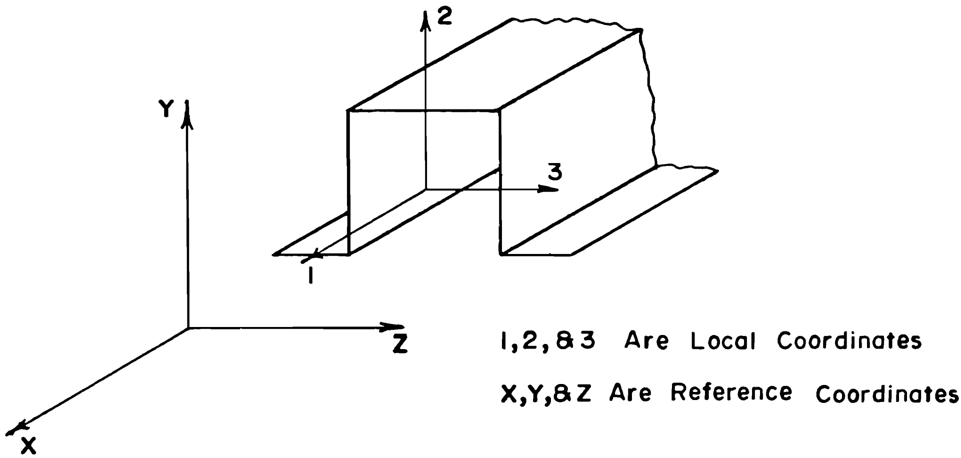

Fig. 5 - Definition of Reference and Local Coordinate Systems

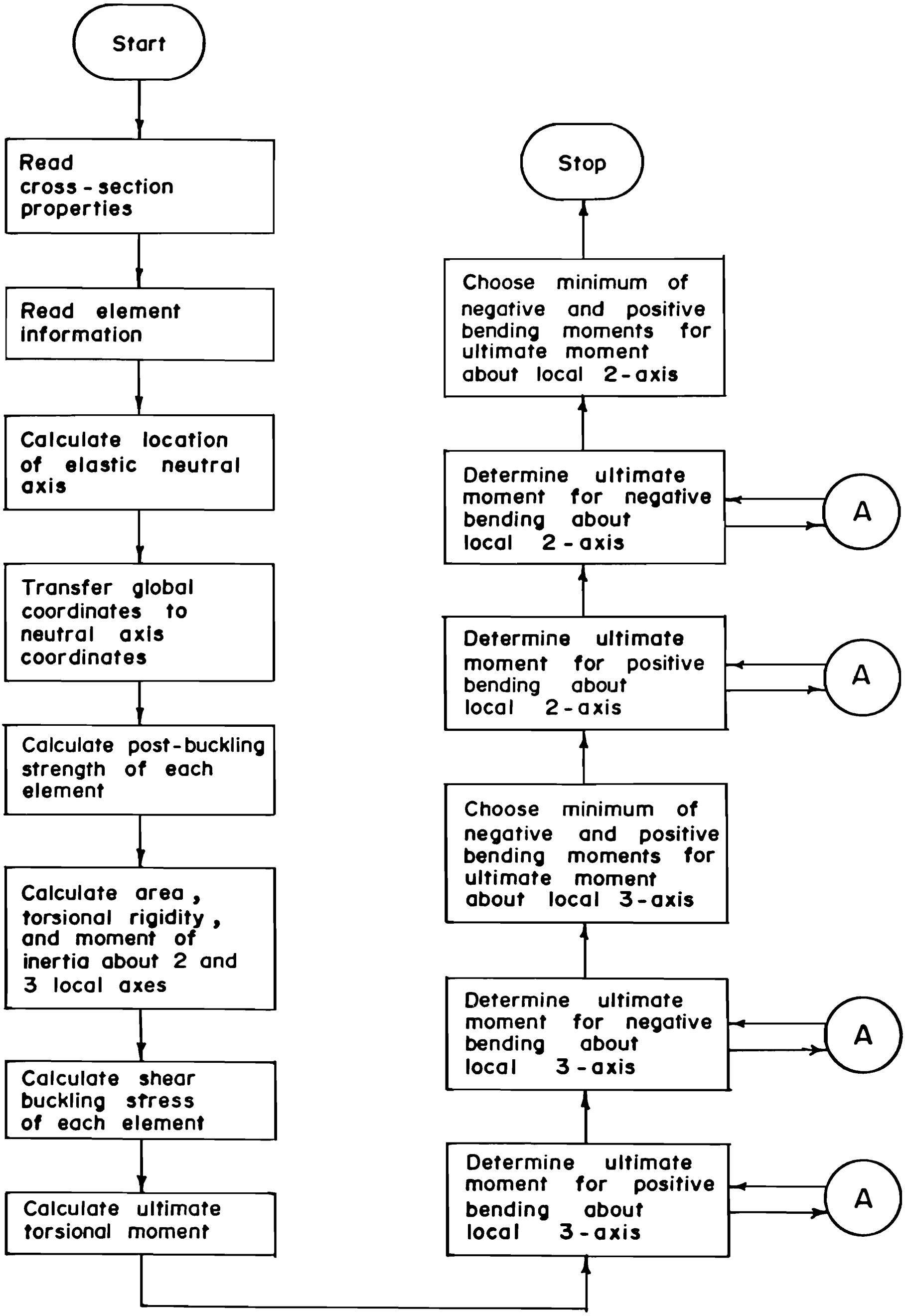

Fig. 6 a - Flow Chart for PROP

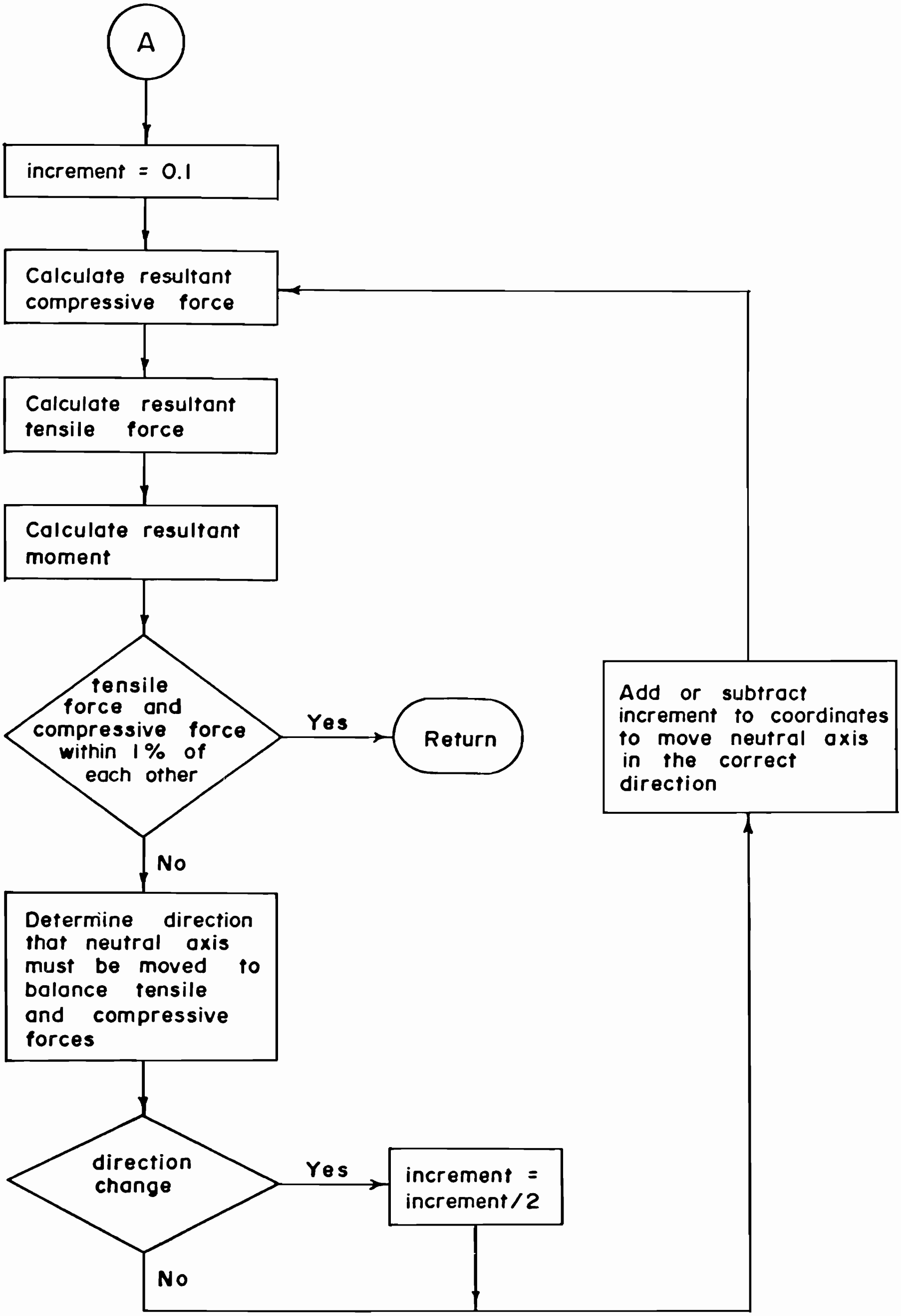

Fig. 6b-Flow Chart for PROP Subroutine

BUS B HAT SECTION

```
NO. OF SECTIONS      =        5
CROSS SECTION TYPE   =        0
  EQ.0, OPEN SECTION
  EQ.1, CLOSED SECTION
YIELD STRESS (KSI)   =     54.0
YOUNG*S MODULUS (KSI)=  30000.0
POISSONS RATIO       =    .3000
```

SECTION NUMBER	ISTIFF	SECTION COORDINATES (INCHES) Z1	Y1	Z2	Y2	T INCHES	R INCHES
1	0	.0000	.0000	.7200	.0000	.0600	.0940
2	1	.7200	.0000	.7200	1.1900	.0600	.0940
3	1	.7200	1.1900	1.7800	1.1900	.0600	.0940
4	1	1.7800	1.1900	1.7800	.0000	.0600	.0940
5	0	1.7800	.0000	2.5000	.0000	.0600	.0940

SECTION NUMBER	FLAT WIDTH INCHES	ULTIMATE STRESS KSI
1	.5960	51.7279
2	.9420	54.0000
3	.8120	54.0000
4	.9420	54.0000
5	.5960	51.7279

SECTION ELASTIC PROPERTIES

AREA IN**2	J(1) IN**4	I(2) IN**4	S(2) IN**3	I(3) IN**4	S(3) IN**3
.29280	.00035	.11824	.09459	.06933	.10810

SECTION PLASTIC PROPERTIES

PM(1) IN-KIPS	Z(1) IN**3	PM(2) IN-KIPS	Z(2) IN**3	PM(3) IN-KIPS	Z(3) IN**3
.2739	.0051	9.0621	.1678	6.9559	.1288

Fig. 7 - PROP's OUTPUT

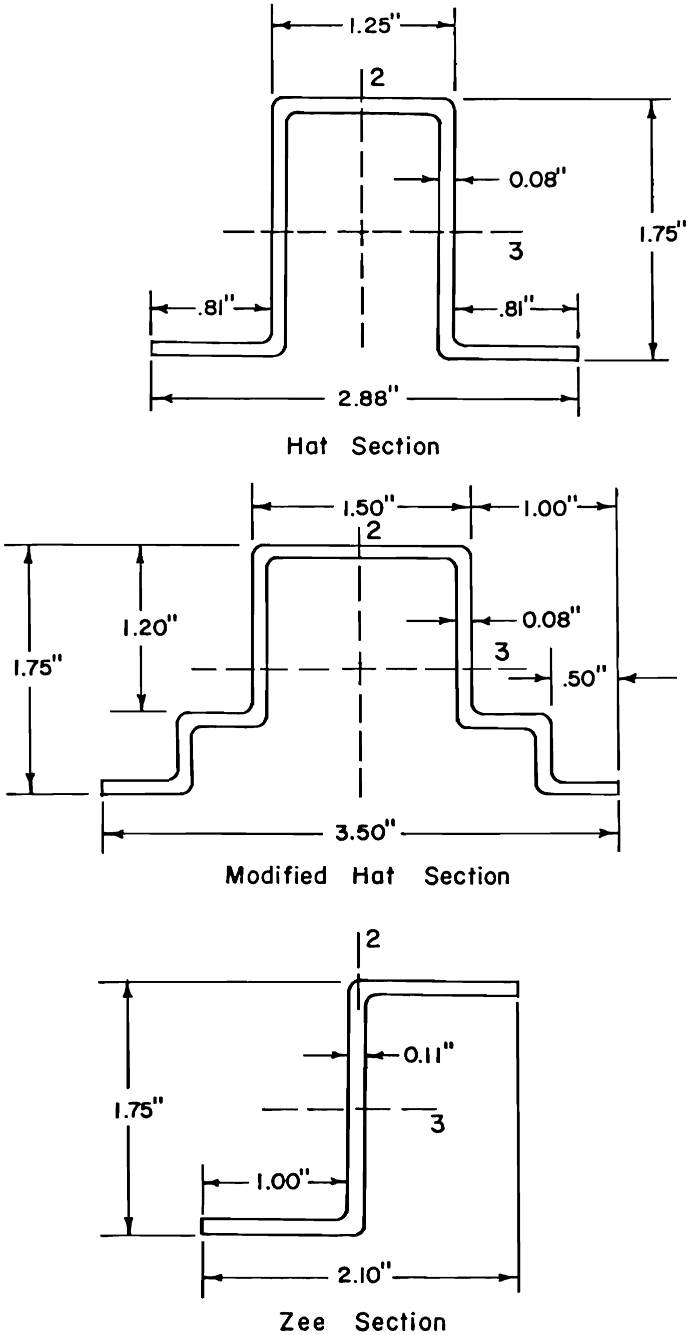

Fig. 8 - Bending Test Specimen Shapes

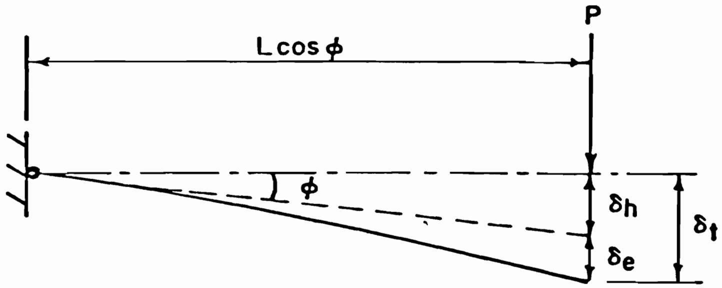

P = applied load

δ_e = elastic deflection

δ_h = deflection due to hinge rotation

δ_t = total deflection

ϕ = hinge rotation

Fig. 9 -Moment-Hinge Rotation Parameters

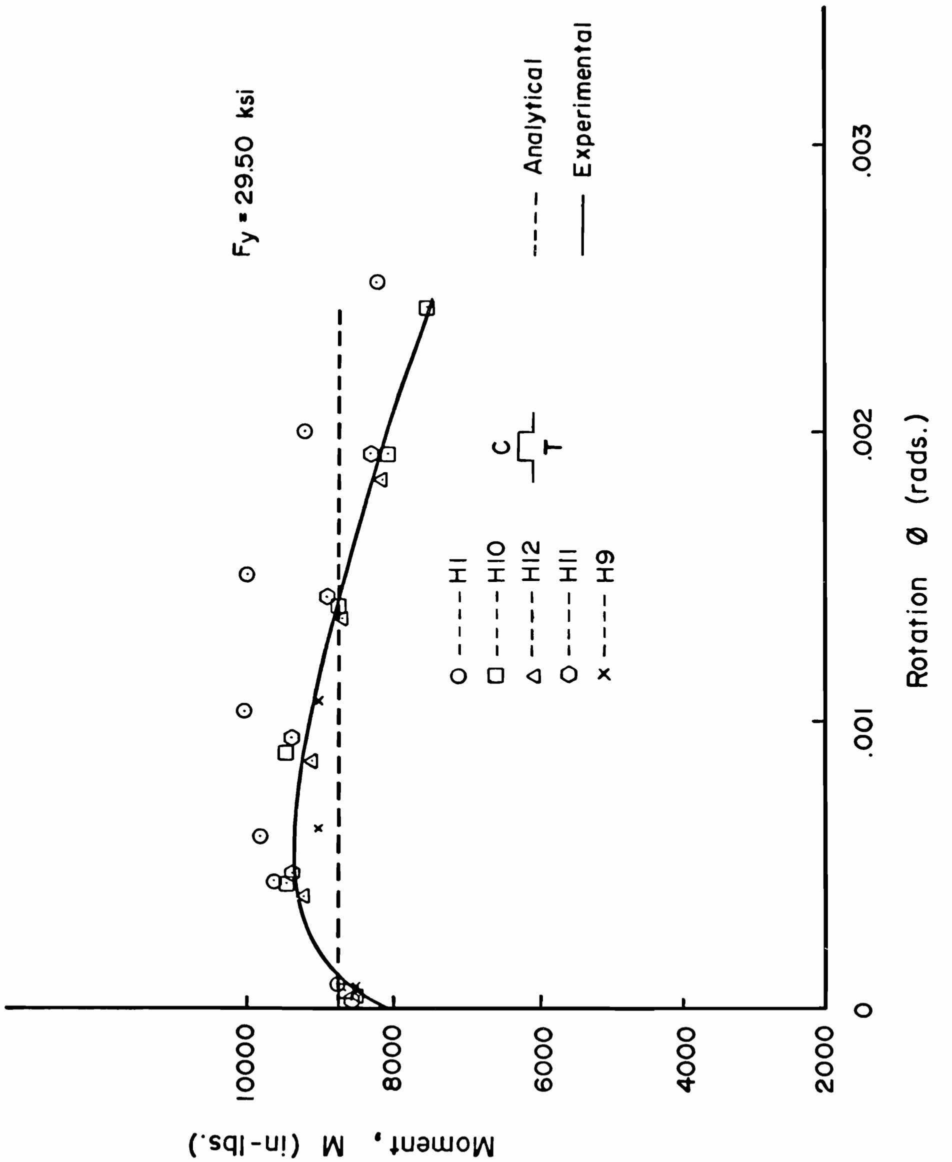

Fig. 10 -Moment vs. Rotation

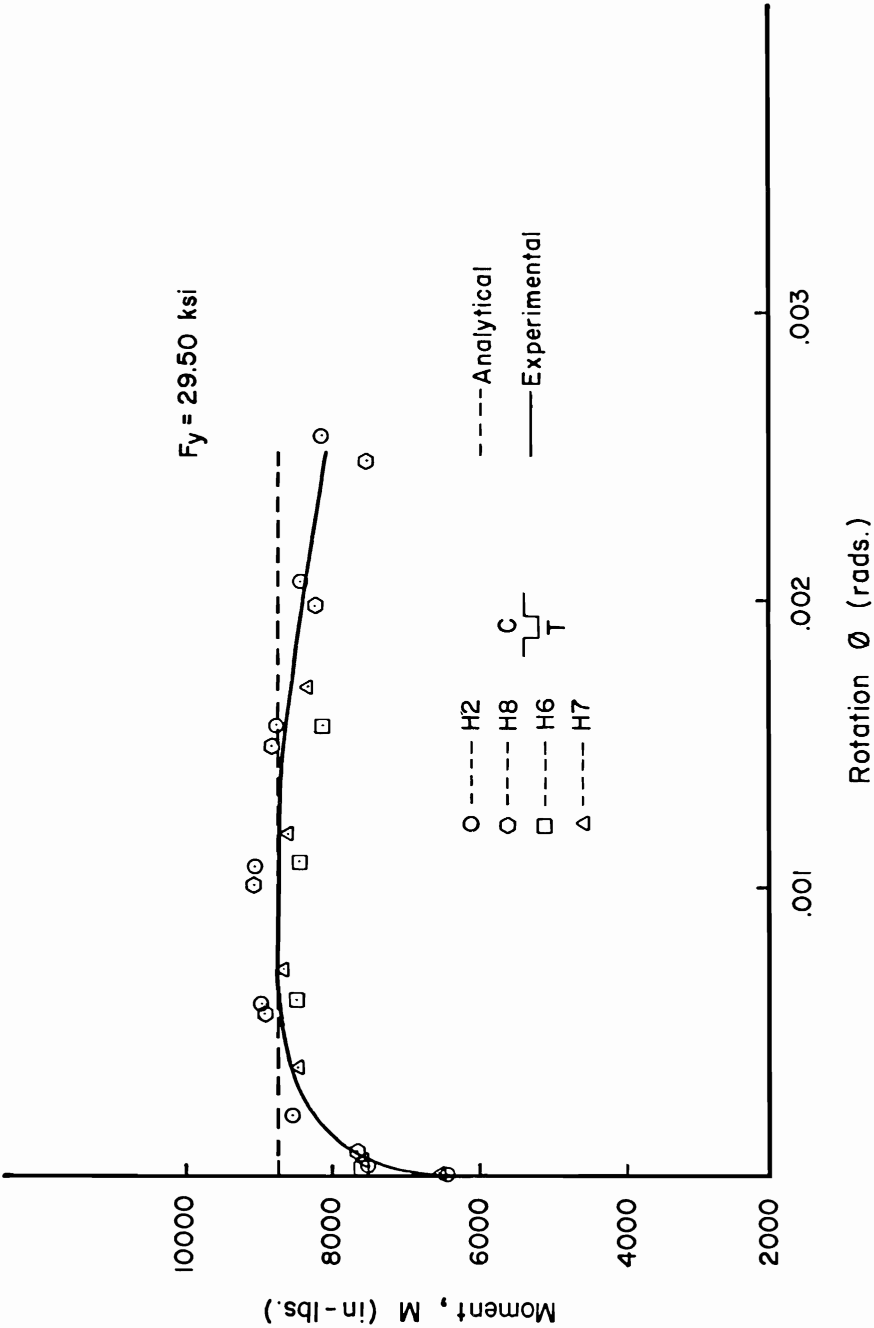

Fig. 11 - Moment vs. Rotation

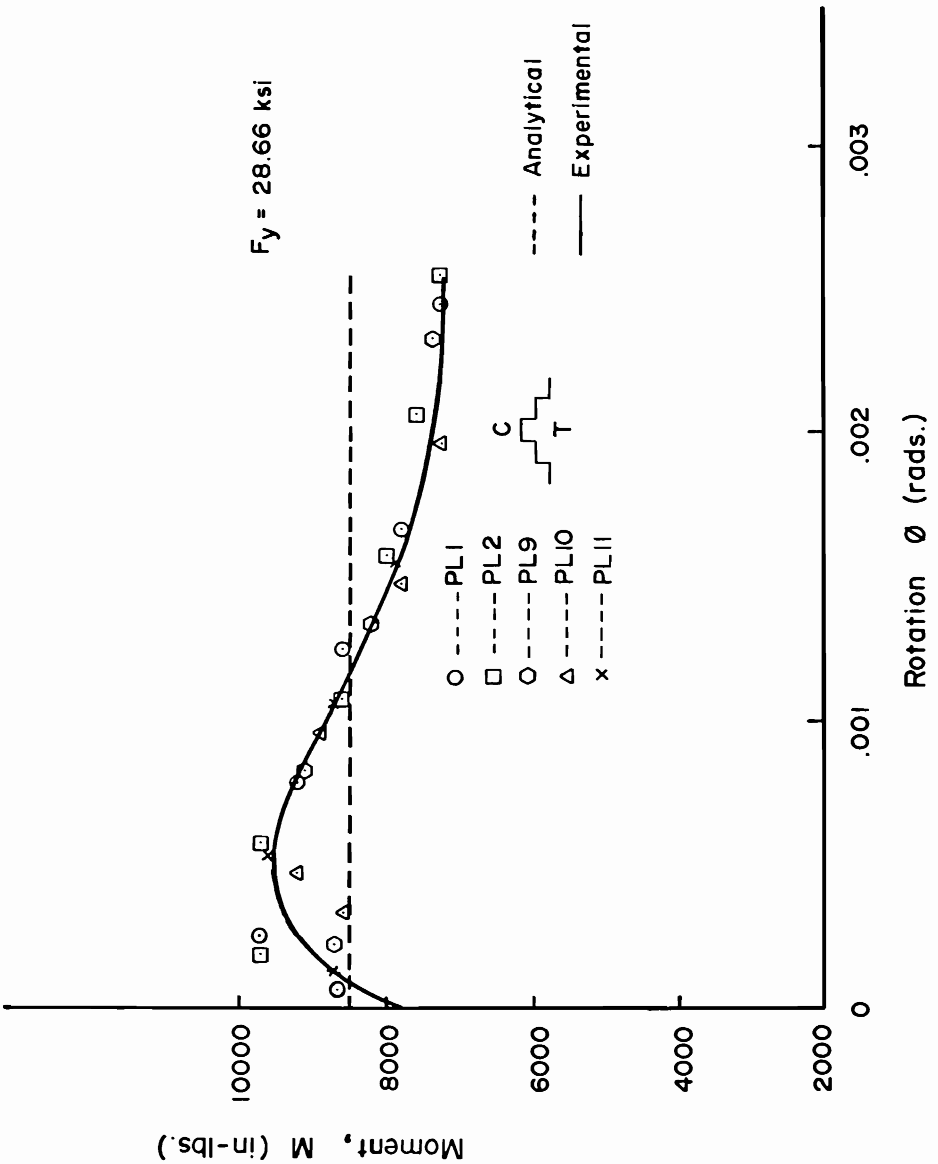

Fig. 12 - Moment vs. Rotation

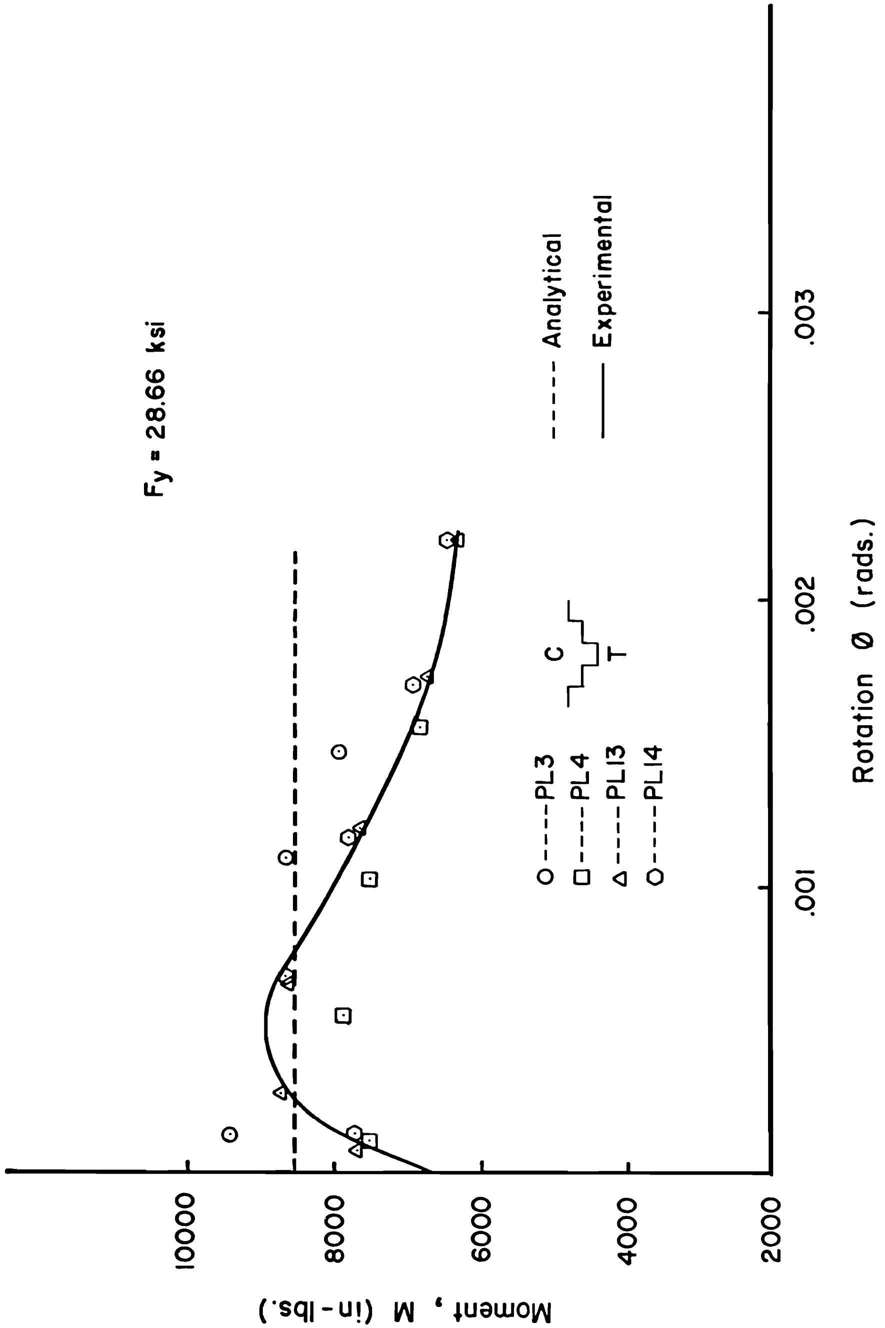

Fig. 13 - Moment vs. Rotation